Liquid Crystals
Publication details, including instructions for authors and subscription information:
http://www.informaworld.com/smpp/title~content=t713926090

Unusual thermal behaviour of mesogens containing an N,N-dialkylaminomethylene lateral substituent

Cecile Canlet

Online publication date: 06 August 2010

To cite this Article Canlet, Cecile(1999) 'Unusual thermal behaviour of mesogens containing an N,N-dialkylaminomethylene lateral substituent', Liquid Crystals, 26: 2, 281 — 289
To link to this Article: DOI: 10.1080/026782999205425
URL: http://dx.doi.org/10.1080/026782999205425

LIQUID CRYSTALS, 1999, VOL. 26, NO. 2, 281–289

Unusual thermal behaviour of mesogens containing an *N*,*N*-dialkylaminomethylene lateral substituent

CÉCILE CANLET, PATRICK JUDEINSTEIN, JEAN-PIERRE BAYLE*
Laboratoire de Chimie Structurale Organique, Université Paris XI. U.R.A. 1384. 91405, Orsay Cedex, France

FRÉDÉRICK ROUSSEL
Laboratoire de Dynamique et Structure des Matériaux Moléculaires, Université du Littoral, U.R.A. 801, MREID, 59140 Dunkerque, France

and BING M. FUNG
Department of Chemistry and Biochemistry, University of Oklahoma, Norman, Oklahoma 73019-0370, USA

(*Received 9 September 1998; accepted 6 October 1998*)

An *N*,*N*-dialkylaminomethylene lateral substituent can be used to reduce the melting temperatures of nematogens having a long rigid core. However, compared with a single lateral alkoxy chain, this lateral substituent does not enhance the thermodynamic stability of the mesophase. DSC curves and optical microscopy show that after melting, a new solid appears in the liquid crystal phase or in the isotropic phase of these compounds. NMR spectra of the nematic phase and of the solid phase show that a thermal reaction releases dialkylamine into the medium and produces a disubstituted 2*H*-indazole in rather good yield. Further heating of each individual mixture leads to a second wide range enantiotropic nematic phase. The purified disubstituted 2*H*-indazole has a larger nematic range and the nematic phase is stable at high temperature, indicating that the 2*H*-indazole motif can be used to build new mesogenic structures. The temperature dependence of the ^{13}C chemical shifts of one of the initial compounds was obtained. The results indicate that the two chains on the nitrogen atom are equivalent and more or less folded back in the same way along the mesogenic core.

1. Introduction

Lateral flexible substituents attached to a fairly long rigid core have the interesting ability to decrease melting temperatures while preserving mesomorphic properties [1–6]. We have investigated several types of lateral substituents: alkoxy chains, substituted benzyloxy fragments and bifurcated alkoxy chains [1, 2, 5, 6]. Our previous NMR studies have revealed that the lateral substituent is folded back along the molecular long axis due to the anisotropic forces encountered in the nematic phase [7–10]. To carry out a systematic study on the influence of the type of lateral chain after the initial investigations of lateral substituents containing the fragments $-OCH_2-$ and $-CH_2-CH-$ [1, 6], we decided to examine the influence of a nitrogen and of its position by using $-NR_2$ and $-CH_2-NR_2$ as lateral fragments (figure 1).

In conventional mesogens, alkyl or alkoxy chains are commonly used as terminal substituents in order to decrease the melting temperatures with the consequence of increasing the thermodynamic stability of the mesophase. The replacement of a carbon or oxygen atom by a nitrogen in the terminal chain generally reduces the mesogenic properties of rod-like molecules [11–13]. This phenomenon is generally attributed to hydrogen bonding [11], electronic delocalization [12], and/or nitrogen lone pair intermolecular interaction [13]. All these factors are detrimental to the liquid crystalline phase and promote the stability of the solid phase.

The problem addressed in this paper is rather simple. Can molecules having an *N*,*N*-dialkylamine fragment in the lateral chain exhibit liquid crystal properties? To answer this question, we present the synthesis of two related series containing a nitrogen atom in the lateral chain. These compounds contain the same core used in our previous series [1, 5, 6], but differ by the position

*Author for correspondence.

Journal of Liquid Crystals ISSN 0267-8292 print/ISSN 1366-5855 online
http://www.tandf.co.uk/JNLS/lct.htm
http://www.taylorandfrancis.com/JNLS/lct.htm

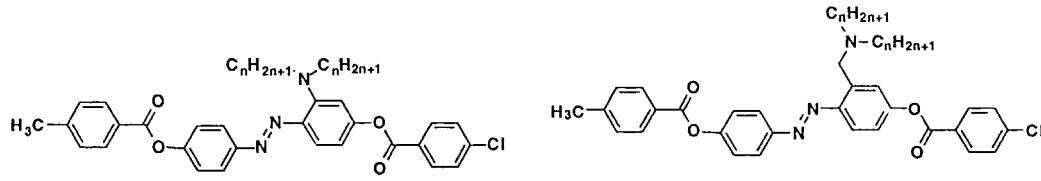

Figure 1. Chemical structures of the two series synthesized.

of the nitrogen atom in the lateral chain. The DSC behaviour of one series is unusual as it is found that on increasing the temperature two nematic phases are separated by a solid form. This unusual behaviour has been investigated by NMR spectroscopy in solution, on the solid and on the nematic phase. In addition, the evolution of the chemical shifts with temperature was obtained in order to have some information on the lateral chain conformations.

2. Experimental

2.1. *Synthesis*

The synthetic scheme for series **II** is presented in figure 2. In the first step, the Schiff 's base was prepared using a classical procedure. It was not isolated and the reduction was performed on the cooled reaction mixture [14]. Then, the methanol was evaporated under vacuum and the boron complex hydrolysed using saturated ammonium chloride solution. The monoalkylated amine was twice extracted into ether and the resulting ethereal phase washed twice with water. After drying over sodium sulphate and evaporating the ether, the crude product was crystallized from ethanol. The second alkylation was carried out in acetonitrile using the method described by Ferry [15]. Two equivalents of alkyl bromide and triethylamine were used in order fully to alkylate the secondary amine. The crude compound was chromatographed on silica gel (60–200 mesh) with ethyl acetate. The substituted aniline hydrochloride used for the diazotization step was obtained through conventional methods [16]. Then, the diazo-coupling was performed, using dioxan as solvent and the phenol under basic conditions [17]. Coupling occurs mainly *para* to the remaining hydroxyl group. After evaporation of dioxan, the mixture was shaken with three portions of ether and the extracts were washed three times with water. After drying and evaporating the solvent, the crude product was chromatographed on silica gel (60–200 mesh) with CH_2Cl_2/ethyl acetate (80/20) and then CH_2Cl_2/methanol as eluents, and the phenol was collected as the

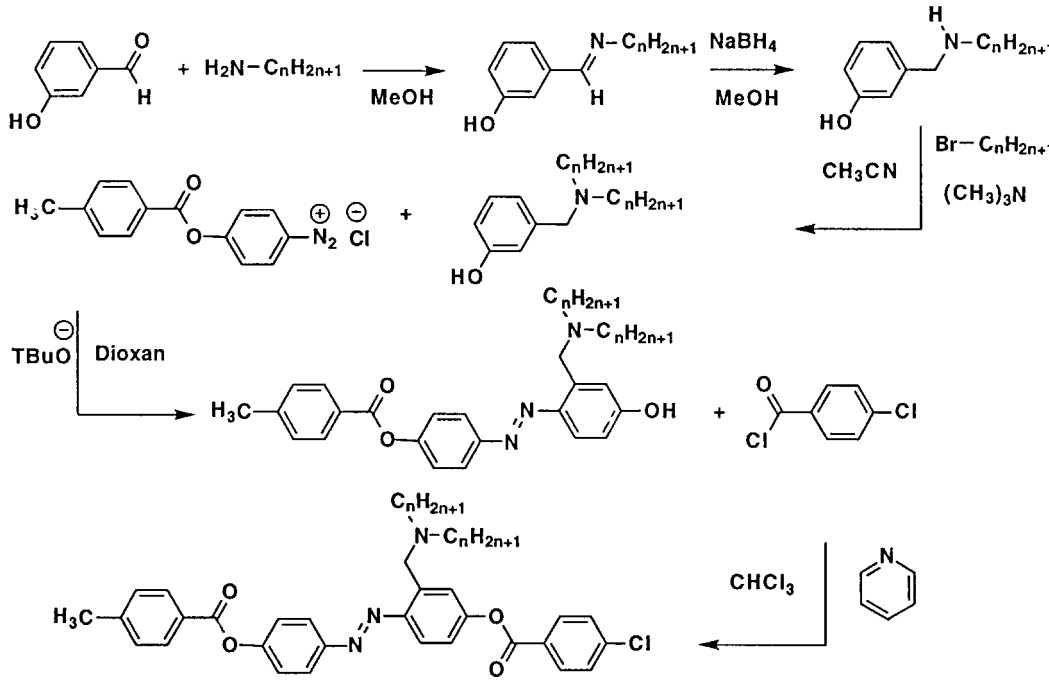

Figure 2. Synthetic scheme for series **II**.

last fraction. Finally, this phenol was esterified with 4-chlorobenzoyl chloride in $CHCl_3$/pyridine as solvent. After acidification, the mixture was shaken with ether and the extract washed twice with acidified water, twice with dilute ammonia and finally twice with water. After chromatography (silica gel 60–200 mesh, eluent CH_2Cl_2, first fraction), the final product was crystallized from a mixture of toluene/ethanol/4-methylpentan-2-one (10/80/10) until constant transition points were obtained. These transition points were measured by DSC (Mettler FP 52) using a heating rate of 10°C min^{-1}. Thermogravimetric analyses (TGA) were performed on a Shimadzu TGA-50H apparatus using a gas flow rate of 70 ml min^{-1} and a heating rate of 2°C min^{-1}.

2.2. *NMR experiments*

Slow spinning ^{13}C NMR experiments on the liquid crystal phase and on solutions were performed using a Varian Unity-400 NMR spectrometer ($B_o = 8.86$ T) equipped with an indirect detection probe manufactured by Narolac Cryogenic Corporation. The sample was put in a standard 5 mm tube and spun along the magnetic field so that the director aligned parallel to the magnetic field. To avoid rf overheating, a 0.8% decoupler duty cycle was used.

High resolution, solid state ^{13}C NMR experiments were performed on a Bruker MSL 200 spectrometer with quadrature detection using a double-tuned coil for ^{13}C and ^{1}H NMR. The crystalline samples were filled into fused zirconia rotors fitted with boron nitride caps and spun at 6 kHz at the magic angle (54.7°). ^{13}C chemical shifts were referenced to the glycine carbonyl signal (assigned at 176.03 ppm) used as external reference. The spectra were obtained using cross-polarization pulse (with a ^{1}H 90° pulse of 4.1 μs), high power decoupling during acquisition (0.03 s acquisition, 3 s recycle delay, 512 scans and 1.2 ms mixing time). Variable temperature CP/MAS NMR experiments were performed in the 30–250°C range using a Eurotherm thermal controller, calibrated using the DABCO, 1,4-diazabicyclo-(2,2,2)-octane, crystal–crystal transition [18].

3. Results and discussion

3.1. *Transition temperatures*

The transition temperatures of the four compounds synthesized in series **I** are given in table 1. A monotropic mesophase with a short nematic range was obtained for the compounds **ND6** and **ND8**, indicating that an *N*,*N*-dialkylamino lateral chain does not promote liquid crystal properties. The thermal behaviour of compounds belonging to series **II** is far more complex.

The DSC curves for **CND4** and **CND6** obtained at a 10°C min^{-1} heating rate are presented in figure 3. The surprising phase transition sequences Cr_1–N–Cr_2–N–I and Cr_1–N–I–Cr_2–N–I were observed for **CND4** and **CND6**, respectively. The transition temperatures and the $\Delta S/R$ values for the four compounds synthesized in series **II** are presented in table 1. An enantiotropic nematic phase was obtained for **CND4**, **CND6** and **CND8**, indicating that the methylene group between the aromatic ring and the bifurcated amino chain is needed for thermodynamic stability of the mesophase. The phase transition sequence for **CND8** is similar to that of **CND6**, but has a much narrower nematic range (figure 3). The compound **CND10** does not exhibit a lower temperature nematic phase: the crystal melts to an isotropic liquid directly. These observations show that the lateral fragment –CH_2–N(R)$_2$ is less favourable for liquid crystal properties than –O–CH(R)$_2$ or –O–R lateral fragments.

It seems that the short CH_2 spacer permits the alignment of the two chains along the core, but the molecular arrangement of the –CH_2–NR_2 lateral fragment in the nematic phase may be different from that observed for a –O–CH(R)$_2$. Molecular modelling performed on a single molecule shows the possibility of two minimized conformations, one with the chains aligned along the core on the same side, and the other on opposite sides (figure 4).

Now let us further discuss the DSC curves and the related microscopic observations (heating rate 10°C min^{-1}) for these compounds. For **CND4**, after melting, a nice schlieren texture characterises the nematic

Table 1. Transition temperatures (in °C) for the two series and $\Delta S/R$ values for series **II**. These values were taken with increasing temperature (heating rate 10°C min^{-1}); dec = decomposition.

Series **I**	Cr	→	I	→	N	Series **II**	Cr_1	→	N	→	I	→	Cr_2	→	N	→	I
ND4	•	148	•	(86)	•	**CND4**	•	106 9.1	•			152.5 – 19	•	231 11.3	•	352 dec	•
ND6	•	109	•	(99)	•	**CND6**	•	73 19.3	•	101 0.2	•	155.5 – 40.2	•	229 9.8	•	354 dec	•
ND8	•	108	•			**CND8**	•	71.5 17.5	•	74.5	•	157 – 34.3	•	229.5 10.6	•	348 dec	•
ND10	•	107	•			**CND10**	•	79 16.3			•	155 – 32.8	•	231 9.9	•	340 dec	•

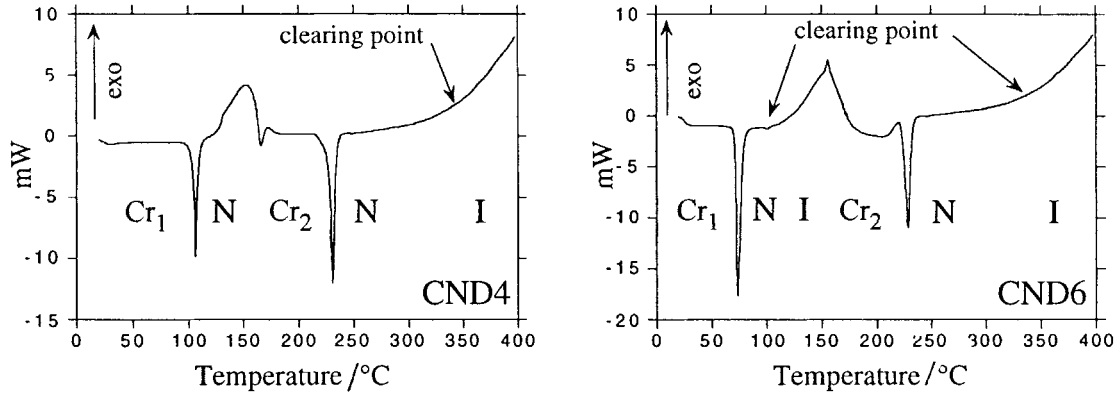

Figure 3. DSC curves for **CND4** and **CND6**, compounds of series **II** (heating rate = 10°C min^{-1}). The high temperature clearing point was observed by optical measurements.

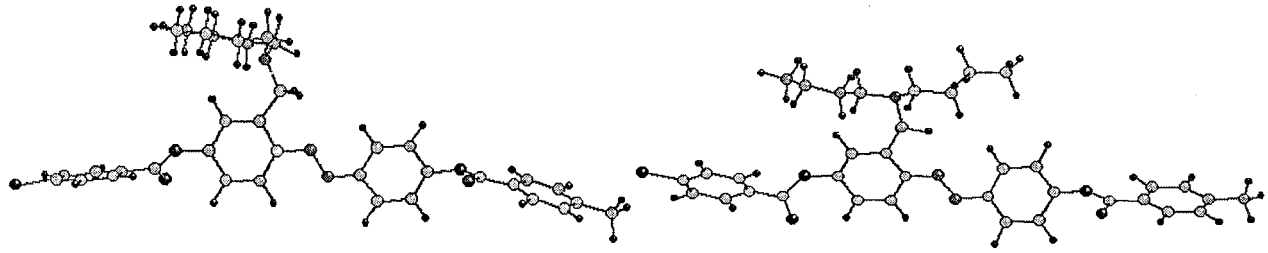

Figure 4. Two minimized conformations of **CND4** implying a folding of the chains along the core: (*a*) on the same side, (*b*) on opposite sides.

phase. At 121°C, crystals started to grow in the nematic phase. This new crystalline phase is related to the broad exothermic peak associated with a large enthalpy in the DSC curve, indicating that there may be a chemical reaction occurring inside the sample. The maximum of this peak is nearly at the same temperature regardless of the chain length. In addition, unlike the other peaks on the DSC curve, the position of this peak is dependent on the temperature ramp. A slower ramp shifts this peak towards lower temperature: for example, the maximum is shifted to 145°C for a rate of 5°C min^{-1}. This gives a clear indication about the thermal activation of the chemical reaction. After this chemical reaction, the microscope film which was originally pale red due to the azo link became completely colourless in the centre, with some brown edges at the outside of the film. From this observation, we can conclude that the chemical reaction involves the breaking of the double bond in the azo linkage. As this internal reaction does not occur in series **I**, we have a strong clue that in addition to the azo bond, the reaction may involve the methylene group between the ring and the *N*-bifurcated chain. At 160°C, a small endothermic peak appeared in the DSC, but there was not much change in the optical appearance of the film. For **CND6**, this sharp peak is replaced by a broad one around 195°C. This broad peak disappears in the **CND8** and **CND10** samples. We will return to the interpretation of this peak later. The new solid melts again at 230 ± 1°C to give a new nematic phase. This temperature is independent of the chain length, and the associated entropy is also quite constant ($\Delta S/R = 10.4 \pm 0.9$). From these experimental facts, we can propose that the reaction is intramolecular and the structure of the new white solid does not depend on the chain length of the starting material. After the second melting, the nematic phase is stable over more than 100°C depending on the sample. The clearing point was not observable on the DSC curve as there was some internal degradation around the clearing temperature.

3.2. ^{13}C *chemical shifts analysis*

Figure 5 shows the ^{13}C NMR spectra of the compound **CND6** under different conditions. Because the intramolecular chemical reaction is thermally activated, a powder sample of **CND6** was introduced directly into the NMR tube in order to avoid effects from any transformation due to the thermal history of the sample. To obtain the spectrum of the nematic phase, figure 5(*b*), the temperature was raised to 80°C, just above the solid–nematic transition. Compared with the spectrum in $CDCl_3$ solution, figure 5(*a*), the aromatic peaks show large positive jumps because of the chemical shift anisotropies caused by the alignment of the nematic sample of positive $\Delta\chi$ due to the four aromatic rings belonging to the core.

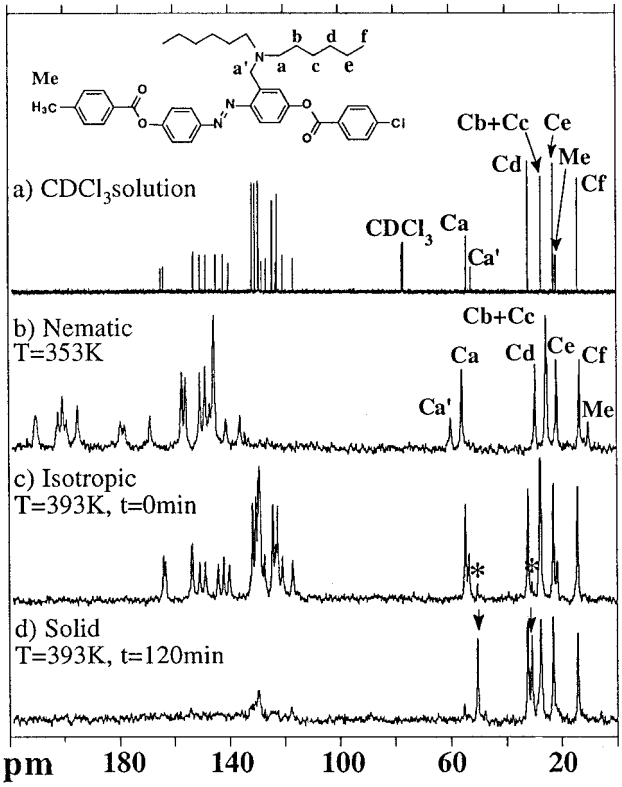

Figure 5. ^{13}C NMR spectra of **CND6** (*a*) in $CDCl_3$, (*b*) in the nematic phase at $T = 353$ K, (*c*) in the isotropic liquid phase at $T = 393$ K and (*d*) in the second solid form at $T = 393$ K after two hours at this temperature. For spectra (*b*), (*c*) and (*d*) 100 scans were acquired on a slowly spinning sample, with a special broadband proton decoupling sequence using a decoupler power of 20 kHz.

In the aliphatic part of the spectrum, the assignment of the solution spectrum below 30 ppm is quite straightforward as the two alkyl chains are equivalent. For the carbons linked to the nitrogen, the intense peak at 54.0 ppm was assigned to the two first carbons belonging to the alkyl chains, Ca. Whereas, the ^{1}H chemical shift of Ha and Ha′ are rather different at 2.52 and 4.15 ppm, respectively; there is only a slight difference between the chemical shifts of the Ca′ (52.4 ppm) and Ca (54.0 ppm) carbons, certainly due to some conformational effects. In the nematic phase, these carbons exhibit a positive jump in their chemical shifts, whereas the other chain carbons and the methyl group attached to the terminal phenyl ring experience the usual negative jump. We will return to the interpretation of these positive jumps of the Ca′ and Ca carbons in the last part of the discussion.

On increasing the temperature slowly, the nematic–isotropic transition was obtained at 94°C, which is far below the transition temperature observed in the DSC curve. This result indicates that even at this low temperature the intramolecular reaction occurs and leads to products which affect the transition temperature. Then, the temperature of the sample was raised further to 120°C and a spectrum was taken every 15 min to analyse the chemical transformation. The first spectrum is presented in figure 5(*c*). This spectrum is quite similar to the one obtained in $CDCl_3$ solution, with the exception that at least two new peaks (marked by asterisks) appear in the aliphatic part due to a compound formed in the intramolecular reaction. At this temperature, the successively recorded spectra show a gradual increase in the two new peaks and a decrease of the peaks in the aromatic region. After two hours at 120°C, the aromatic part has almost completely disappeared and the new peaks indicated by the arrows are preponderant and have the same intensities as the other aliphatic peaks, figure 5(*d*). Because there was insufficient decoupling power and no MAS, the ^{13}C peaks of the new solid would be too broad to be observed. This is essentially the case for the aromatic signals. However, the narrow peaks in the aliphatic region indicate that a liquid is likely to be present, and it may be due to another product formed in the intramolecular reaction.

In the isotropic solution and in the nematic phase, two peaks are observed in the 50 ppm region corresponding to the two different carbons directly attached to the nitrogen atom, Ca and Ca′, figures 5(*a*) and 5(*b*). In spectrum (*d*), a single peak is observed in the same region. Moreover, six peaks are observed corresponding to six different carbons in the chains. This means that Cb and Cc carbons no longer have the same chemical shifts. It is well known that the chemical shifts of the carbons near a nitrogen atom depend on its degree of substitution [17]. Quantitatively, the α effect decreases with the number of chains substituted on the nitrogen atom, whereas the β effect increases, no γ effect is observed, and the δ effect is very small. In the spectrum we observed a decrease of the Ca carbon chemical shift, an increase of the Cb chemical shift and essentially no change in the Cc chemical shift. This is a good indication that in the liquid compound, the nitrogen atom substitution has decreased. Thus, we conclude that the Ph–CH_2–NR_2 bond breaks to release *N*,*N*-dialkylamine in the intramolecular reaction.

In order to verify this hypothesis, we have performed CPMAS experiments on the solid compound produced from **CND4**. Figure 6 presents the CPMAS spectra at room temperature of the starting red solid (*b*) and the white solid (*d*) obtained by heating the sample for two hours at 150°C. For comparison, the spectrum in $CDCl_3$ solution (*a*) and the MAS spectrum of the isotropic melt at 120°C (*c*) are also shown. As expected, spectrum (*b*) shows four distinct massifs in the aliphatic region. The broad peak around 54 ppm corresponds to the overlapping of the Ca and Ca′ carbons. In the isotropic

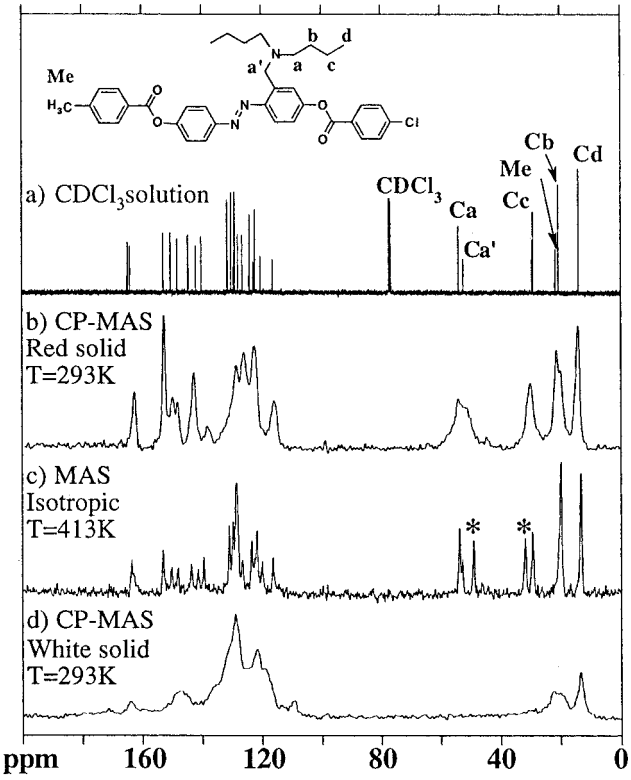

Figure 6. ^{13}C NMR spectra of **CND4** (*a*) in $CDCl_3$ solution, (*b*) in the starting solid at $T = 293$ K, (*c*) in the isotropic liquid phase at $T = 413$ K and (*d*) in the second solid form at $T = 293$ K after heating the sample for two hours at $T = 423$ K. For spectra (*b*), (*c*) and (*d*), 2048 scans were acquired on a fast spinning sample. CP conditions were used for spectra (*b*) and (*d*) with a proton decoupling power of 45 kHz.

spectrum (*c*), obtained by simple MAS with high proton decoupler power (45 kHz), two more peaks marked by asterisks are present at 49.6 and 32.5 ppm and, respectively, can be assigned to the Ca and Cb carbons belonging to the *N*,*N*-dibutylamine moiety. These chemical shifts should be compared to 54.4 and 29.9 ppm for Ca and Cc belonging to the starting material, showing changes due to different nitrogen atom substitutions. After heating the spinning rotor at 150°C for two hours in the magnet, the rotor was cooled down to room temperature and the CPMAS spectrum was recorded under the same conditions as spectrum (*b*). No peak was present in the 50–60 ppm region, figure 6(*d*). This clearly indicates that the white solid no longer contains any lateral substituent. This is consistent with the observation that the Cr_2–N transition for all the homologues, regardless of the chain length of the original compound, are nearly identical. The boiling points of dibutylamine, dihexylamine, dioctylamine and didecylamine are 159°C, 192–195°C, 297–298°C and >350°C, respectively. The endothermic peaks observed at 160 and 195°C in the DSC curves of **CND4** and **CND6** correspond to the boiling of the dialkylamines generated.

3.3. *Structure of the new mesogenic core*

It is known that a diazonium salt can react with an activated methyl or methylene group to give the related indazole [20–22] in good yield, through the reaction:

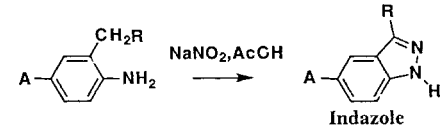

The corresponding azo compounds have also been used as a source of indazoles, even though they are less reactive. If a methyl group is present in the position *ortho* to the azo linkage, the cyclization can occur in the presence of a base and a nitroso compound if the methyl group is activated by a nitro group in the *para*-position [23–25]:

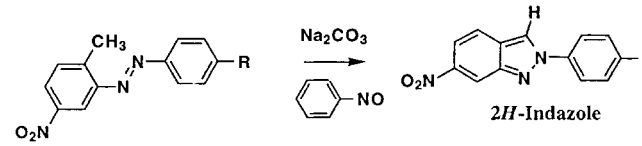

The product belongs to the group of 2*H*-indazoles, and the formula of these derivatives presents an *ortho*-quinonoid fragment. Nevertheless, these compounds are best regarded as delocalized aromatic systems rather than as dienes with localized bonding [25]. Other compounds containing a reactive methylene group can undergo such cyclization by simple heating. In 1904, Freundler showed that an azo compound having an alkoxymethylene group in the *ortho*-position can experience an intramolecular cyclisation around 170–180°C [26–28]:

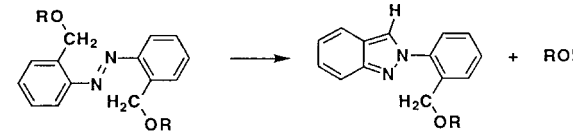

We did not find in the literature any example with an *ortho*-*N*,*N*-dialkylaminomethylene fragment. Nevertheless, as the dialkylamine is a reasonably good leaving group, a similar reaction is possible for our compounds. It is interesting to note that, in the isotropic melt, the temperature needed for the cyclization is almost identical to that observed by Freundler. In order to verify the loss of the dialkyl part, we have performed thermogravimetric analysis (TGA) on the four compounds using a dynamic method. A typical thermogram recorded with an air flow rate of 70 ml min^{-1} and a temperature ramp of 2°C min^{-1} is presented in figure 7.

As can be seen, the intramolecular reaction starts at 105°C and ends at 175°C with a minimum of the first derivative at 140°C. After that the sample continues to

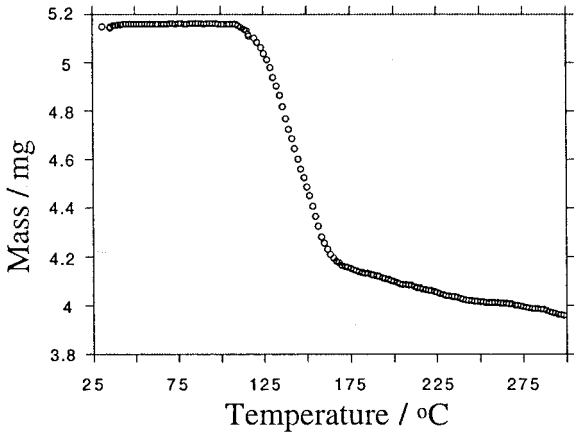

Figure 7. TGA curve of **CND4**: flow rate = 70 ml min^{-1}, temperature ramp = 2°C min^{-1}.

lose weight, certainly due to some thermal degradation. During the cyclization, the loss of mass is 20.1%, which is very near the expected 21.1% which gives a good indication of the yield in the intramolecular reaction. Isothermal measurements were made at 170°C under air and nitrogen, and the losses were 20.6 and 20.7%, respectively, which indicates the reliability of the dynamic measurement and that the thermal reaction does not involve oxidative degradation.

Thus, we can propose the mechanism of formation and the formula of the second compound.

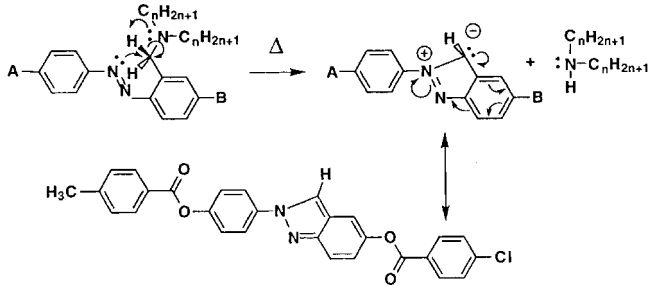

The ^{1}H NMR spectra of the starting material **CND4** and the crude disubstituted 2*H*-indazole compound in deuteriated acetone are presented in figure 8. Only the peaks above 3.5 ppm are shown.

The 2*H*-indazole was obtained after heating 100 mg of pure **CND4** at 140°C for two hours and then washing the solid with dichloromethane. The disubstituted 2*H*-indazole compound is rather insoluble in many organic solvents. Thus, after filtration, a small amount of the solid was dissolved in deuteriated acetone. Figure 8(*b*) shows that the –CH_2–N signal diminishes together with the appearance of a signal at 9.0 ppm which can be attributed to the hydrogen involved in the newly formed double bond. The pattern and the chemical shifts of the hydrogens belonging to the aromatic rings do not change drastically. This is not surprising, as the central heterocyclic core has to be considered as a delocalized aromatic system rather than as dienes with localized bonding.

The mesogenic 2*H*-indazole was purified by several recrystallizations from DMSO and the transition temperatures T_{CrN} and T_{NI} were found to be 235°C and 413°C (dec.), respectively; the values were reproducible. This shows that the core derived in the 2*H*-indazole is suitable for liquid crystal properties, even if the core is certainly slightly bent due to the non-colinearity of the N–C and C–O bonds on each side of the indazole structure. The angle between these two bonds has been measured as 155° in a related compound [29].

3.4. *Chemical shift changes in the nematic phase*

In our initial attempt to perform measurements of the ^{13}C chemical shifts on the pure azo compound in the nematic phase, a problem was encountered. Above 80°C, the intramolecular reaction in the liquid crystal phase started to take place, yielding the dialkylated amine as one of the products, with consequent drastic narrowing the nematic range. It is interesting to note that the intramolecular reaction proceeds quite rapidly at lower

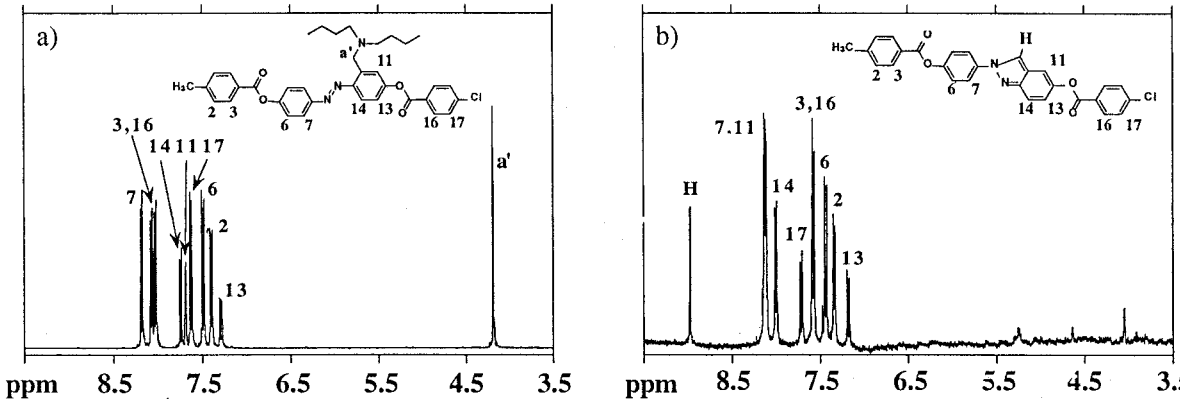

Figure 8. ^{1}H NMR spectra in CD_3COCD_3 solution of (*a*) **CND4**, (*b*) the crude indazole.

temperatures in the nematic phase of the compounds. The packing in the nematic phase would certainly help the reaction by decreasing molecular disordering [30]. In order to avoid the intramolecular cyclization, we chose to decrease the nematic–isotropic transition by mixing the compound **CDN6** with **ZLI1184** [*trans*-1-cyano-4-(*trans*-4-propylcyclohexyl)cyclohexane]. Several mixtures were prepared at different concentrations of **ZLI1184**. The chemical shift behaviour is nearly identical for all the mixtures.

The evolution of the ^{13}C chemical shifts of the aliphatic and aromatic carbons in **CND6** as a function of temperature is presented in figure 9 for the mixture **CDN6/ZLI1184** (68.1/31.9 mass ratio). In the isotropic phase, the two chains are chemically equivalent and their chemical shifts are identical. This also seems to be the case in the nematic phase. In figure 9, the two chemically non-equivalent carbons Ca and Ca′ directly linked to the nitrogen experience a positive jump at T_{NI} when the compound changes from isotropic to nematic phase, whereas the other carbons in the chain show negative jumps.

As already noticed in our previous work, the signs of the jumps in the ^{13}C chemical shifts at the isotropic–nematic transition give valuable information on the mean conformation of the methyloxy or benzyloxy fragment [8]. For a terminal chain, each CH_2 fragment, as well as the terminal CH_3 group, experiences a negative jump at T_{NI} as a result of the averaging of the chemical shift tensor and the bond order parameter over all the populated conformations. In contrast, when a lateral methyl is present on an aromatic ring, its chemical shift experiences a positive jump at the transition from isotropic to nematic. This is due to the positive C–H bond order parameter. The C–H bonds of Ca′ have a geometry similar to that of a lateral methyl substituent, which would explain the positive jump observed for its chemical shift. For lateral alkoxy chains, we have shown that the first CH_2 (second atom within the chain) in the lateral chain possess a positive jump due to the folding back of this fragment within the nematic phase; the second CH_2 (third atom within the chain) exhibits a tiny negative or no obvious jump, and the subsequent CH_2 groups show the usual negative jump [8]. All these changes can be explained by the adaptation of a *gauche*-conformation of the C_{ring}–O–C–C fragment in the folding of the chain. In the present case, as the third atom in the chains (Ca) presents a small positive jump, the mean conformation

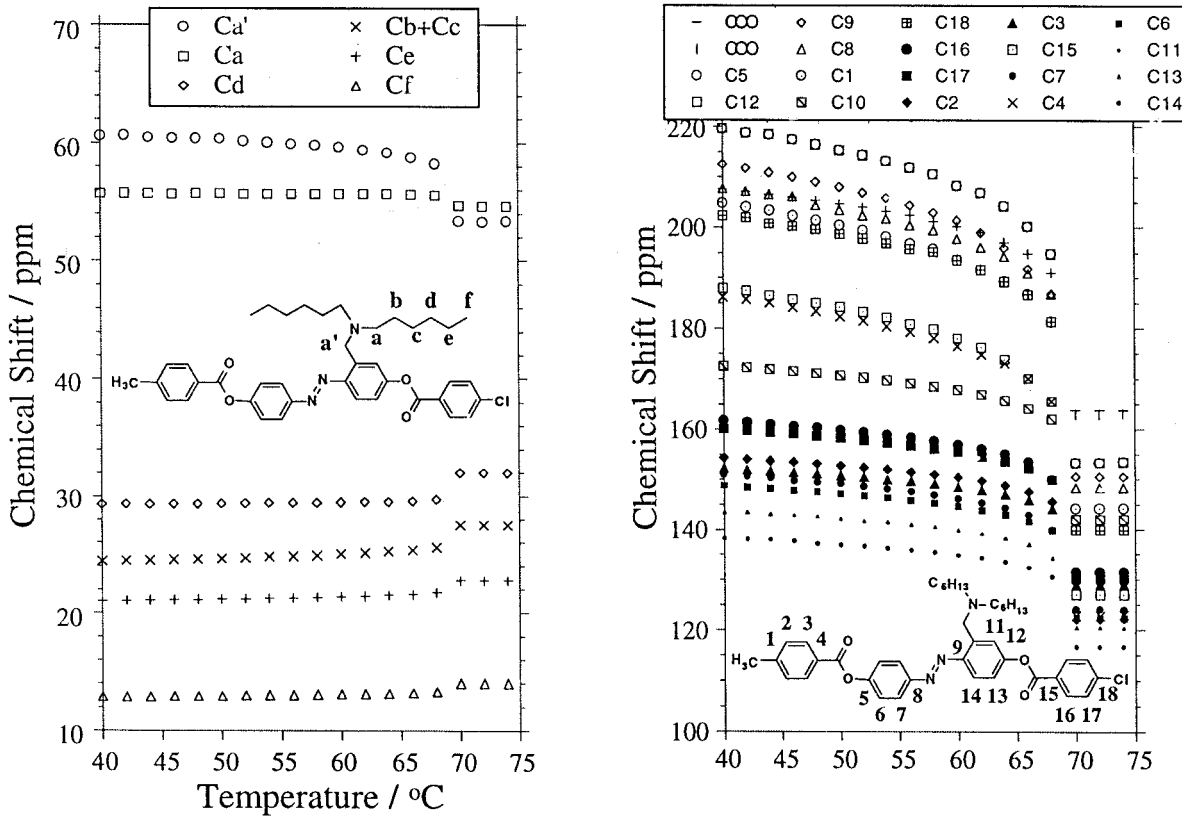

Figure 9. Evolution of the aliphatic and aromatic chemical shifts with temperature for the mixture **CDN6/ZLI1184** (68.1/31.9 mass ratio).

of this carbon has to be different from those of the subsequent carbons along the chain. The conformation depicted in figure 4(*a*) has to be preferred with the two chains folded along the core on the same side.

For the aromatic carbons, the ^{13}C chemical shifts do not present any unusual behaviour. All the quaternary carbons along the major axis exhibits the largest anisotropic chemical shifts.

5. Conclusion

We have synthesized four new compounds, each containing four aromatic rings in the main core and a lateral *N*,*N*-dialkylated aminomethylene fragment on one of the inner aromatic rings. The three first members of the series containing two butyl, hexyl or octyl chains grafted on the lateral nitrogen atom, respectively, exhibit an enantiotropic mesophase. The mean conformation of the aliphatic chains and the aromatic rings has been studied by applying ^{13}C NMR techniques. The carbons having the same position in the bifurcated chain are equivalent and these two chains are folded back along the mesogenic core, involving a *gauche*-conformation for the first fragment. The two lateral chains are more or less aligned with the molecular long axis. Upon heating in the nematic phase or in the isotropic melt, all the compounds give a new solid phase at nearly the same temperature. This exothermic reaction is an internal cyclization with the loss of the dialkylamine fragment. ^{13}C NMR in the solid phase and in the nematic phase was used to probe the reaction. The solid formed at high temperature is a disubstituted 2*H*-indazole which, amazingly, exhibits a large range nematic phase stable at high temperatures. Despite the fact that the core of the molecule is slightly bent, the 2*H*-indazole fragment can act as an interesting rigid part for the building of new mesogenic molecules.

The work of B.M.F. was supported by the US National Science Foundation under grant number DMR-9700680. Grateful thanks are due to Dr E. Lafontaine for the solid state NMR spectra.

References

[1] Perez, F., Bayle, J.-P., and Fung, B. M., 1996, *New J. Chem.*, **20,** 537.
[2] Perez, F., Judeinstein, P., Bayle, J.-P., Roussel, F., and Fung, B. M., 1997, *Liq. Cryst.*, **22,** 711.
[3] Jacobi, A., and Weissflog, W., 1997, *Liq. Cryst.*, **22,** 107.
[4] Bezborodov, V. S., and Petrov, V. F., 1997, *Liq. Cryst.*, **23,** 771.
[5] Perez, F., Judeinstein, P., Bayle, J.-P., Allouchi, H., Cotrait, M., Roussel, F., and Fung, B. M., 1998, *Liq. Cryst.*, **24,** 627.
[6] Canlet, C., Judeinstein, P., Bayle, J.-P., Roussel, F., and Fung, B. M., 1998, *New J. Chem.*, 211.
[7] Perez, F., Bayle, J.-P., and Fung, B. M., 1996, *New J. Chem.*, **20,** 537.
[8] Perez, F., Berdagué, P., Judeinstein, P., Bayle, J.-P., Allouchi, H., Chasseau, D., Cotrait, M., and Lafontaine, E., 1995, *Liq. Cryst.*, **19,** 1015.
[9] Perez, F., Berdague, P., Bayle, J.-P., Brauniger, T., Khan, M., Ho, M. S., and Fung, B. M., 1997, *New J. Chem.*, **21,** 1283.
[10] Perez, F., Bayle, J.-P., Allouchi, H., Belaraaj, A., Cotrait, M., and Lafontaine, E., 1998, *New J. Chem.* (in the press).
[11] Culling, P., Gray, G. W., and Lewis, D., 1960, *J. chem. Soc.*, 2699.
[12] Schroeder, D. C., and Schroeder, J. P., 1976, *J. org. Chem.*, **41,** 2566.
[13] McMillan, J. H., and Labes, M. M., 1979, *Mol. Cryst. liq. Cryst.*, **55,** 61.
[14] Schellenborg, K. A., 1963, *J. org. Chem.*, **28,** 3259.
[15] Buck, J., and Ferry, C. W., 1943, *Org. Synth.*, Vol. II, 290.
[16] Nose, A., and Kudo, T., 1981, *Chem. Phar. Bull.*, **29,** 1159.
[17] Perez, F., Judeinstein, P., and Bayle, J.-P., 1995, *New J. Chem.*, **19,** 1015.
[18] Haw, J. F., 1988, *Anal. Chem.*, **559A,** 60.
[19] Kalinowski, H.-O., Berger, S., and Braun, S., 1988, in *Carbon-13 NMR Spectroscopy* (J. Wiley), p. 221.
[20] Cava, M. P., Noguchi, I., and Buck, K. T., 1973, *J. org. Chem.*, **38,** 2394.
[21] Fusco, R., Marchesini, A., and Sannicolo, F., 1987, *J. heterocycl. Chem.*, **24,** 773.
[22] Bartsch, R., and Yang, I.-W., 1984, *J. heterocycl. Chem.*, **21,** 1063.
[23] Chardonnens, L., and Buchs, M., 1940, *Helv. Chim. Acta*, **23,** 1399.
[24] Chardonnens, L., and Heinrich, P., 1946, *Helv. Chim. Acta*, **29,** 872.
[25] Behr, L. C., 1967, in *Heterocyclic Compounds* (J. Wiley), p. 289.
[26] Freundler, P., 1903, *Bull. Soc. Chim.*, **29,** 742.
[27] Freundler, P., 1904, *Bull. Soc. Chim.*, **31,** 863.
[28] Freundler, P., 1904, *Bull. Soc. Chim.*, **31,** 868.
[29] Nan'ya, S., Katsuraya, K., Maekawa, E., Kondo, K., and Eguchi, S., 1987, *J. heterocycl. Chem.*, **24,** 971.
[30] Leigh, W. J., 1991, in *Liquid Crystals, Applications and Uses*, edited by B. Bahadur, Vol. 2 (World Scientific), p. 357.